Dynamical Behavior of Rotating Machinery in Non-Stationary Conditions: Simulation and Experimental Results

Nicolò Bachschmid and Steven Chatterton

Abstract Condition monitoring of rotating machinery is generally performed in *stationary* conditions or quasi-stationary conditions. Assuming linearity of the system its dynamic behaviour can be simulated in the frequency domain. Simulated results are then compared to measured results and the comparison allows to apply model based diagnostic procedures. As soon as the system presents strong non-linearity, simulation must be performed in the time domain, including also iterative procedures, which may become cumbersome. When the dynamic behaviour of linear or non-linear systems in non-stationary conditions is simulated, the time domain integration must be necessarily used. Accuracy of simulated results gets weaker; comparison with measured results for diagnostic purposes becomes difficult or ineffective; model based diagnostic approach seems not applicable. Monitoring of machines in "strong" *non-stationary* conditions is generally performed only by means of accurate signal analysis, without modelling the machine or the process. In this paper the simulation of some typical behaviour of rotating machines in weak or strong non-stationary conditions in the time domain is presented and discussed. Some experimental results are also presented and compared to simulations. Further examples of systems with strong non-linearity, that in stationary conditions exhibit non-stationary vibrations, are also given.

Keywords Blade Flutter Instability · Blade Vibration · Condition Monitoring · Friction Contact Model · Non-Stationary Conditions · Rotating Machinery · Rotor Rubbing · Steam Whirl Instability

N. Bachschmid (✉) · S. Chatterton
Department of Mechanical Engineering, Politecnico di Milano, Via G. La Masa 1 20156 Milan, Italy
e-mail: Nicolo.Bachschmid@polimi.it

G. Dalpiaz et al. (eds.), *Advances in Condition Monitoring of Machinery in Non-Stationary Operations*, Lecture Notes in Mechanical Engineering,
DOI: 10.1007/978-3-642-39348-8_1,

1 Introduction

Continuous condition monitoring of rotating machinery by means of vibration measurements is a common praxis in all kind of industrial plants. The data collected and the comparison with reference data allow to perform the surveillance of the machine, to detect malfunctioning conditions and to trigger alarms or shut downs. In intelligent monitoring systems these data can be processed in order to enable the use of automatic diagnostic procedures. Among these the model based diagnostic procedure, that allows to compare measured results with calculated ones obtained by means of models of the machine and of the malfunctions, seems to be the most promising procedure. In stationary conditions this procedure proved to be highly effective when data are available in many different quasi-stationary (or steady state) operating conditions, typically during the long lasting run-down transients of turbo-groups which are considered a sequence of steady state operating conditions at different rotational speeds. Linearity of the system must be assumed, simulations are made in the frequency domain, and the model based diagnostic procedure is then developed in the frequency domain. As soon as the system becomes non-linear, although being quasi-stationary, this approach is not anymore accurate or even not applicable, depending on the strength of the non-linearity. The simulation of highly non-linear systems must be effected necessarily in the time domain. For smaller or weaker non-linearity also iterative procedures in the frequency domain and the harmonic balance approach can be used.

When the condition of the machine is non-stationary, time domain simulation is generally needed (instead of frequency domain) in order to enable the model to follow the changing condition of the machine.

Non-stationary conditions may be generated by:

1. Rapidly changing the rotational speed or the frequency of excitation
2. Changing the excitation amplitude and frequency
3. Changing system parameters
4. Instability
5. Systems with strong non-linearity (which with stationary excitation exhibit non-stationary motion).

Some of these changes in non-stationary condition may be slow, some others are rapid.

When changes are slow and the system is linear, the approximation of considering discrete steps in time in which the condition is considered steady or stationary (and the vibrations are then calculated in the frequency domain), can be used, which is enormously convenient for computer time. The model based diagnostic approach in the frequency domain can then be used.

Conversely, when changes are rapid, time domain integration must be necessarily used.

The simulation in the time domain of systems modeled by means of 3D finite elements with rather refined mesh, and still more when some non-linearity is

present (like friction contacts for instance), may become so cumbersome that simulations are not anymore affordable. Modal reduction can then be used for the linear part of the system for strongly reducing the degrees of freedom: with few degrees of freedom time domain integration is then affordable.

One of the problems in monitoring machines in non-stationary conditions is certainly the definition of a reference situation. The actual transient conditions of the machine should be identical to the reference conditions (e.g. same speed and thermal transient, same initial conditions and so on), to allow a comparison and define the deviation from normal behavior and therefore the malfunctioning condition. Otherwise only an accurate model can predict the behavior in different transient conditions, which could be a very difficult task.

A series of examples of simulations (sometimes compared to experimental results) will be given and discussed in the following.

2 Simulation of Transient Behavior of Rotating Machinery Driven by Electric Motors

In this example the start up of a three-phase electrical motor driving a centrifugal pump under no load, modeled with finite beam elements (one torsional degree of freedom per node) and concentrated mass and moments of inertia of the impeller, is simulated. The start up torque time history is given by the electric motor manufacturer. Figure 1 shows the driving torque (bottom diagram) and the results obtained as rotation, velocity or speed, acceleration as typical example of Runge–Kutta time integration.

Of course also torsional deflections are calculated in each element of the finite element model, from relative rotations between the element nodes, from which maximum stresses can be evaluated and compared to the material strength. Such kind of calculation is always required for shaft lines in which electrical machines (generators or motors) are present. Generally the worst conditions are the torsional vibrations excited by short circuits, where the torque may have peaks higher even by one order of magnitude with respect to rated torque. When a torsional natural frequency is excited during this transient severe stresses may appear in some section of the shaft line and shaft strength must be checked. Fortunately this is a transient event and material fatigue may not be considered.

3 Simulation of Transient Behavior of Vibrations of Blades During Steam Turbine Run-up Transient

This example is taken from [1]. The analyzed blade row is the last stage (conventionally called L-0) of a low pressure (LP) steam turbine, composed by 12

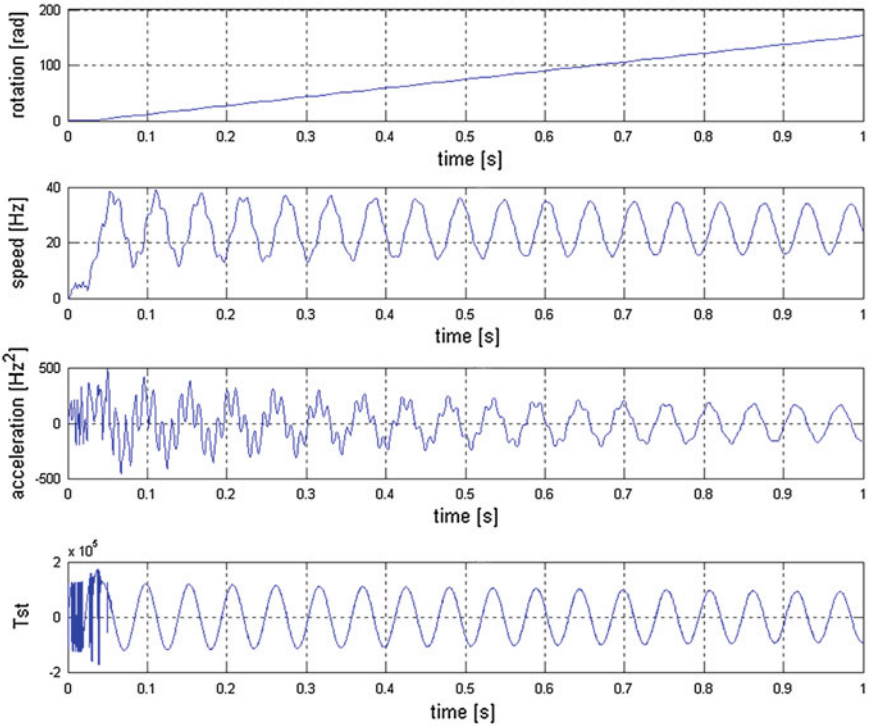

Fig. 1 Start up transient of electric motor driven pump evaluated in one node of the f.e. model

packs of 10 blades each. The blades are grouped in packs of 10 blades by welded shrouds on the tip of the blades and snubbers or lashing wires at an intermediate length of the blade. The first vibrating mode of the pack, which corresponds to an in-phase tangential motion of the blades, has a numerical frequency of 115 Hz. This frequency could be excited in resonance with an engine order 3 at a rotational speed of 2,300 rpm during the run-up of the turbine. This is exactly what happened during the run-up of the machine on the plant, as can be seen from the experimental vibrations reported in Fig. 2. The excitation comes from a non uniform static pressure distribution around the rotating blade row which has apparently a rather strong 3rd harmonic component in the Fourier expansion of the steam pressure around the circumference.

Figure 2 shows the vibration time histories of the first blade of each of the 12 groups as function of the rotational speed during the speed rise between 2,207 and 2,440 rpm which occurred in 7s (with an acceleration of 3.48 rad/sec^2). For the shaft lateral vibration measurement the acceleration is sufficiently low to consider the transient as a sequence of steady state conditions at different rotational speeds. Records were obtained by means of a tip-timing measurement system. Colors indicate phase of vibration with respect to the 1xrev. reference, and show typical phase rotation by passing resonance. Natural frequencies, damping and even

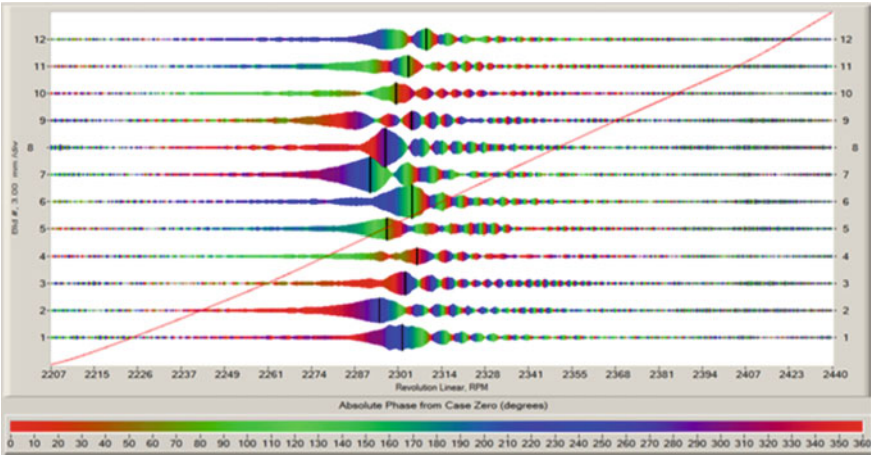

Fig. 2 12 blade pack vibration time histories passing a resonant frequency

excitation seem to be slightly different from pack to pack, due to manufacturing and assembling tolerances, and to some irregularity in the excitation. Being the excitation a 3rd engine order (with a 3xrev. exciting frequency) its acceleration is 10.45 rad/s^2 (three times the rotational acceleration). The effect of this rather high acceleration is clearly visible in the graph: the maximum peak is followed by a series of smaller peaks due to a beating phenomenon between natural and exciting frequency. From this experimental record it is possible to identify both the excitation strength and the modal damping of the blade pack, which are both unknown.

A one d.o.f. modal model of the pack has been build: the stiffness of the pack for this tangential deflection has been defined by applying static tangential unit loads to a finite element model of the blade pack and evaluating the deflections. The modal mass has been deduced from known natural frequency. The modal damping has been defined by comparing the time histories calculated with different values of damping ratios, and unit excitation, to the experimental curves: best fitting defines the modal damping. These time histories are obtained with the usual Runge–Kutta time integration. Being the system linear the time history shapes are independent from intensity of excitation. These curves are shown in Fig. 3: in

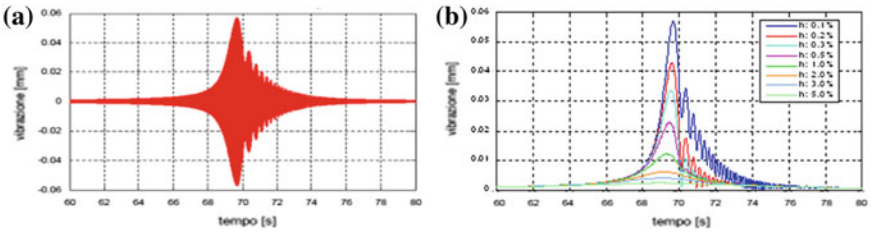

Fig. 3 **a** Vibration time history; **b** Vibration amplitude time histories for different damping ratios

Fig. 3a one generic time history and in Fig. 3b the vibration amplitude as function of time for different modal damping ratios. Resulting best fitting has been found for modal damping between 0.2 and 0.3 % for the different packs.

Maximum amplitude with unit excitation (1 N) and 0.2 % damping ratio in stationary conditions would have been 63 μm, to be compared to 42 μm reached during transient excitation. With this damping ratio and measured vibration amplitude of 2 mm then also the excitation amplitude of the blade pack has been evaluated by proportionality: its value resulted something less than 50 N.

This example shows that system identification is possible with very simple tools also for non-stationary conditions. Also the monitoring of blade vibration by means of tip timing measuring system, for detecting cracks in blade roots, which affect natural frequencies and vibration amplitude, could be possible provided that the acceleration and operating condition of the machine are exactly the same in each run-up transient.

4 Simulation of Blade Rows with Non-Linear Contact Conditions: Single Blade Modeled as 1 d.o.f. System

This example is taken from [2]. A complete integrally shrouded blade row with gaps between shrouds has been modeled by means of 1 d.o.f. per blade modal model representing its first vibration mode, and with non-linear spring and dampers for simulating the contact force between shrouds. Strong model reduction is strictly necessary for having acceptable computer time in calculating blade row behavior. Some gap is allowed between shrouds, harmonic excitation close to resonance is applied and resulting vibrations are calculated. The real blade mounted on a test block and its f.e.m. model showing its first vibration mode are represented in Fig. 4b, and the circular reduced model of the complete row composed of 120 blades is shown in Fig. 4a.

Due to non-linearity time step integration has to be used, and vibrations can result with some chaos, as it is shown in Fig. 5, where vibration time histories of a single blade are represented in two different excitation conditions. The red curve indicates the behavior when shrouds are never in contact (in case of high gap between shrouds) and black curve indicates the resulting vibrations when shrouds get in contact. The contact state (0 open and 1 closed) is indicated by the blue line below in two graphs one for each side of the shroud.

Diagram of Fig. 5a shows the start up transient from stand still before reaching a steady state in resonant conditions: the contact between shrouds reduces consistently the vibration amplitudes with respect to the case with blades with non-contacting shrouds. Diagram of Fig. 5b shows a longer transient in non resonant conditions, where contact generates random vibrations with higher amplitudes than blades with non-contacting shrouds. Other blades behave similarly.

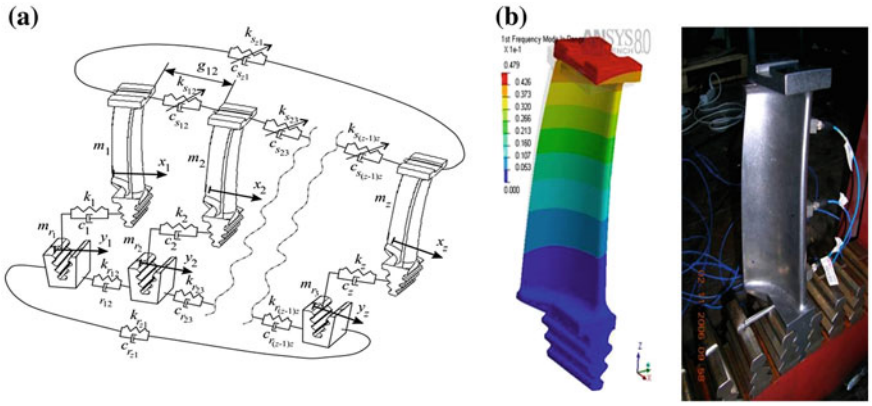

Fig. 4 Integrally shrouded blade row with non-linear contact conditions between shrouds

This is an example of a system in stationary conditions, with a stationary excitation, that behaves randomly which is not exactly a stationary condition, due to a high contact non-linearity. Monitoring blade vibrations in these conditions (which are stationary random) would be rather difficult, despite the fact that in the vibration spectra as that one shown in Fig. 6, some lines are repetitive and could be used as reference.

The contact model is obviously rather rough. More realistic models require to define in the contact area parts which are in sticking contact, parts which are in a sliding or micro-sliding contact, and parts which are separated, which are function of friction coefficient and of contact normal and tangential stiffness, which in turn depend on penetration depth. A more realistic calculation is presented in the following.

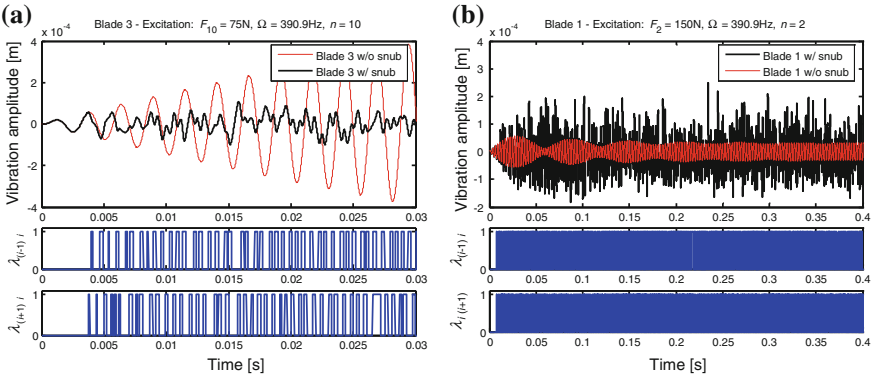

Fig. 5 Vibration behavior of one blade of the row in different excitation conditions: **a** in resonance; **b** out of resonance

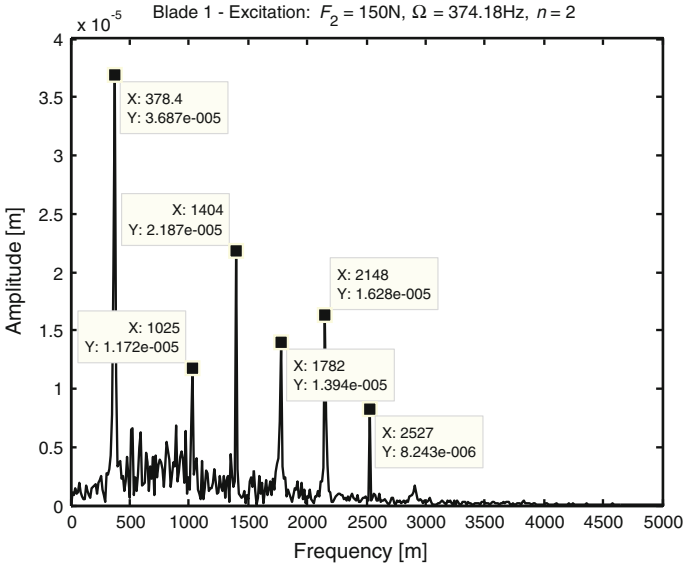

Fig. 6 Vibration spectrum of blade 1 of the row excited slightly out of resonance

5 Simulation of Groups of Blades with Non-Linear Friction Contact Conditions: Full Finite Element Models for Blades and Shrouds

Different contact conditions with different contact forces between shrouds of a group of blades mounted on a test block (represented in Fig. 7a) have been simulated. The complete analysis is described in detail in [3] In the experimental tests, the two internal blades (blades 2 and 3) will be excited independently by two shakers with the same force, but with a predetermined phase shift in order to simulate different engine order excitations of the blade row in the machine. A screw on the top of the test block generates between shrouds a suitable preload contact force which will be measured by a load cell. Resonant conditions are investigated by simulations for emphasizing dynamical behavior. Load has been applied in three steps: first the load from bottom to the blade roots (for simulating centrifugal load on blades in the stationary test rig), then the contact preload, and finally the harmonic loads on the blades, possibly in resonance. Contact pressure distribution after the two load steps are also shown in Fig. 7b.

The natural frequencies and a frequency response curve have been previously calculated with a linear model (with frictionless no separation contact between shrouds). The maximum vibration amplitude in resonance (511 Hz) and out of phase excitation resulted 30 μm. The non-linear frequency response with friction contact on all shrouds has to be calculated at the end of 150 load cycles for getting a steady state solution. Therefore the computation of the steady state response of

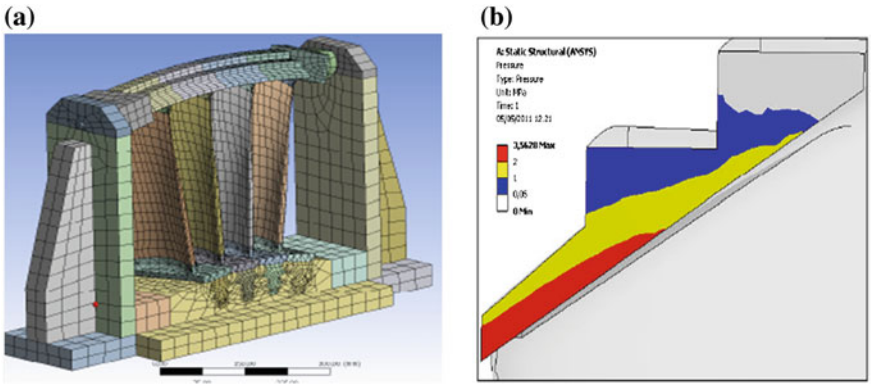

Fig. 7 **a** F.e.m. model of the test rig with the group of blades **b** resulting shroud contact pressure distribution

the system in correspondence of one exciting frequency requires up to a maximum of 150 h with a cluster of 32 processors. The results are stored only for the last load step (when steady state condition has been reached) and may require up to 90 GByte. Several hours are required to download these results on a workstation.

Some results are shown in Fig. 8a: vibration amplitude has been reduced dramatically due to the increased stiffness in sticking contact areas, and to friction in micro-slipping contact in the remaining contact areas: only 1.8 μm (Fig. 8a), with a phase delay of 45° between the two excitations applied to the blades, was the maximum amplitude compared to the frictionless result of 30 μm. Vibrations are sinusoidal like the excitation force, apparently no non-linear behavior is visible.

But when contact preload is reduced (Fig. 8b) then non-linear behavior appears, vibration is periodical but non sinusoidal, slipping is enhanced and vibration amplitude reduces consistently. And when friction coefficient is reduced from 0.2 to 0.1 (Fig. 8c) vibration remains periodical, amplitude as well as slipping increases. These behaviors are steady state.

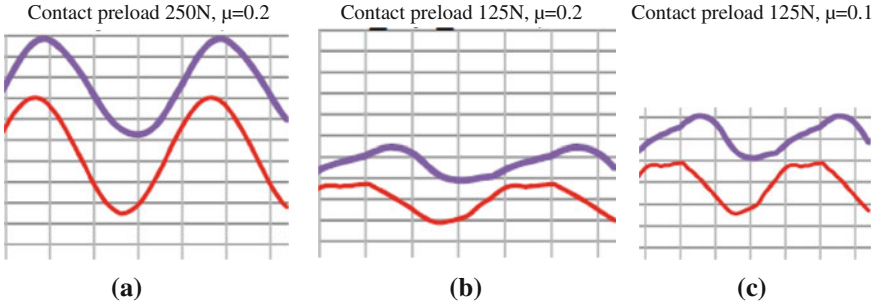

Fig. 8 Vibrations of the two blades in different contact conditions (blade 2 in *red* and blade 3 in *blue*)

Reducing further the friction coefficient to 0.01 vibration becomes non periodic, and seems to be unstable but limited in amplitude. A kind of random vibration in low frequency range (sub-harmonic with respect to the excitation frequency) builds up. This behavior is an unsteady condition, despite the fact that the mechanical system as well as the excitation is stationary.

Of course it must be checked (best by experiments) if this behavior is a physical instability or if it could be attributed to a numerical instability.

6 Simulation of Rotor Rubbing Conditions at Constant Speed

An interesting example of non-stationary thermal state of a shaft due to rubbing which generates non-stationary vibrations concerns the so called spiral vibrations. This behavior is described in detail in [4]. The heat which develops during rubbing of a rotating shaft against a stator, generates a bow of the shaft which evolves in time, and the changing bow generates vibrations. This is a typical example of a rotating shaft in non-stationary conditions. This behavior should therefore be studied in the time domain. But vibrations are 1xrev., at rotational speed frequency of 50 Hz, and should be calculated in time domain with time steps of a fraction (e.g. 1/100) of the rotation period (let's therefore consider a suitable time step of 0.0002 s). Heat distribution due to the friction force evolves slowly, the rotor bow shows appreciable changes in time periods of minutes, depending on shaft diameter. A suitable time step for evaluating the thermal state of the rotor could be 1 min. Using a time step of 0.0002 s for calculating a transient of hours would be a cumbersome exercise. Therefore we can consider the rotor state in each minute of the thermal transient as stationary for the vibrations, and calculate the changes in vibration of the shaft in the frequency domain. This has been done in the simulation of the so-called spiral vibrations of a rotor. The designation comes from the fact that the measured vibration vector moves on a spiral path in a polar plot.

Figure 9 shows the model of the shaft, beam elements for calculating shaft vibrations and a refined mesh in radial, tangential and axial directions for heat distribution calculation. The flow chart of Fig. 10 represents the cyclic computational procedure in time/frequency domain. In time domain the rub conditions are defined from initial conditions and from actual vibration behavior and the consequent temperature and strain distribution is calculated. In the frequency domain strains are converted in equivalent bending moments that are applied to the shaft as well as the contact forces (and the original unbalance) for calculating its vibrations. Then the loop is repeated.

Results of the calculation are shown in Fig. 11a as a 3D plot for the temperature at the contacting point which migrates in circumferential direction as function of time. The contact point migrates because the thermal bow contributes to the original unbalance in generating the vibration excitation: the resulting vibration

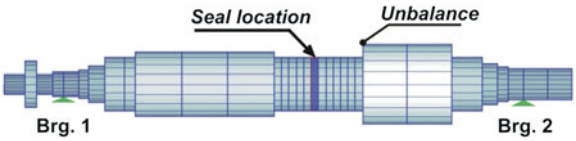

Fig. 9 Model of the shaft of a HP-IP steam turbine rubbing at seal location

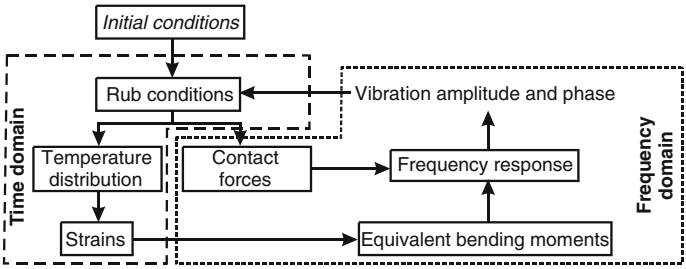

Fig. 10 Flow chart of the computation method in time/frequency domain

vector changes direction as well as the contact point. Figure 11b shows the thermal power introduced in the rotor due to friction as function of time steps.

Figure 12a then shows the equivalent bending moments at a certain time instant as calculated from thermal strains, which simulate the bow. Finally Fig. 12b shows the polar plot of the spiral vibration (amplitude and phase) that could be measured in correspondence of the bearings of the shaft, at the rotational speed of 3,300 rpm. In this case it is an unstable spiral, because vibrations are increasing. But also stable spiral vibrations can occur, when amplitude of vibration decreases and finally the contact is lost. After that when heat is again uniformly distributed the unbalance will force the shaft to rub again and the cycle repeats. This occurs at a rotational speed of 3,500 rpm, as it is shown in Fig. 13a.

Finally also an experimental result compared to the simulated one is represented in Fig. 13b. The rubbing occurred close to a bearing in correspondence of a oil seal ring in a 50 MW turbo-group.

7 Experimental Evidence of Full Annular Rubs During a Speed Transient, and Model Based Identification of the Generated Changing Bow

This is an example of a turbo-group (schematically represented in Fig. 14) in which the HP-IP rotor experienced a full annular rub during a run-down transient approaching its 1st natural lateral frequency: therefore we have a non-stationary speed and a non-stationary thermal state. The complete case history is described in

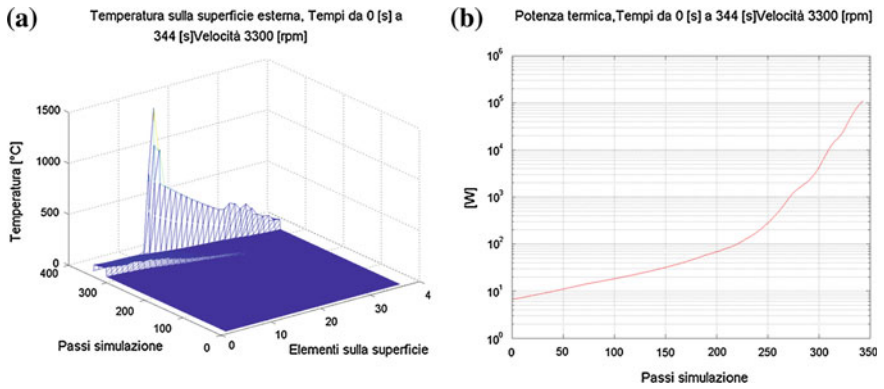

Fig. 11 **a** Temperatures on rotor surface; **b** Thermal power evolution in time

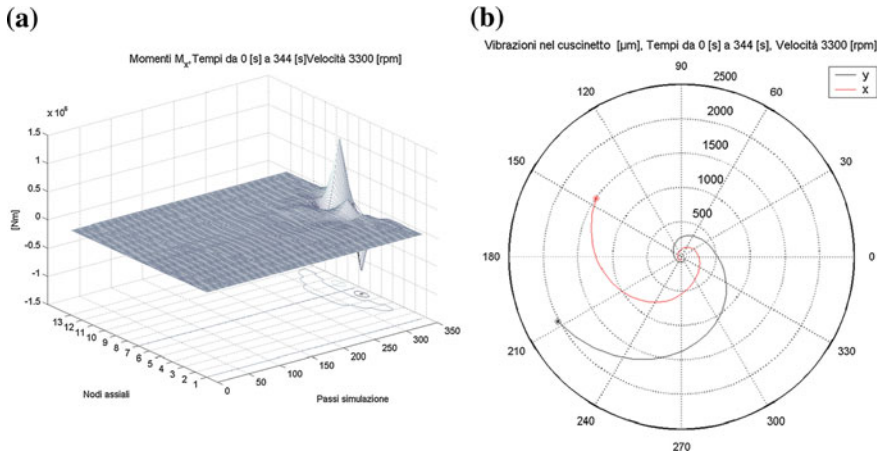

Fig. 12 **a** Equivalent bending moments simulating bow; **b** Unstable spiral vibration (3,300 rpm)

detail in [5]. The run-down transient occurs, as usual for big turbo-groups, with a sufficient low deceleration so that the transient can be considered as a sequence of steady state conditions. As in previous example also here the thermal transient is rather slow: the generated bow is slowly changing, resulting vibrations are changing slowly and this behavior can be analyzed by a sequence of steps with different speed and heat conditions, in which vibrations can be simulated in the frequency domain.

Measured vibrations in the two bearings of the rubbing turbine are reported in the two Bode diagrams of Fig. 15. The run-down had been interrupted as vibration amplitude reached alarm levels close to the shaft first critical speed, rotational speed was increased to get out of the critical speed and trying to relax the thermal stresses and straighten the shaft. Since this attempt was unsuccessful, the run-down

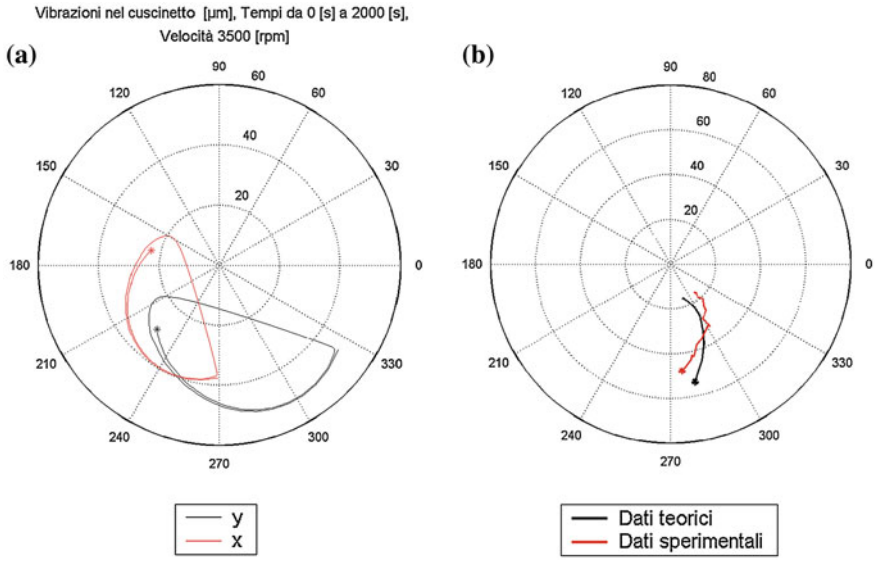

Fig. 13 **a** Stable cyclic spiral vibrations; **b** Measured and simulated spiral vibrations

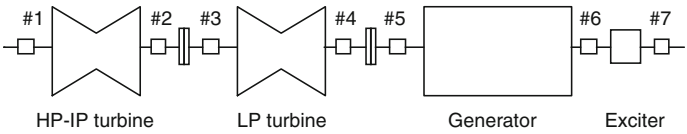

Fig. 14 Turbo-group with a rub in HP-IP turbine rotor

was completed in rubbing conditions for a consistent part of the run-down. At minimum speed a consistent thermal bow remained as can be seen from residual amplitude at 500 rpm in bearing 2. That a severe full annular rub occurred can be deduced also from phase changes: analyzing amplitude and phase of the 1xrev vibration amplitudes measured in the two bearings in between 1500 and 1800 rpm, we have at same rotational speed completely different vibration vectors (with different amplitude and different phase). This is due to the changing thermal bow generated by the rubbing friction.

In order to verify where the rubbing occurred with the aid of the beam element model of the machine, from vibrations in the bearings during the run-down from 1,800 rpm the amount and the location of the rub and the developing bow were identified.

Figure 16 shows the finite element model of the shaft line (composed of the steam turbines only) and the model used to represent the thermal bow by equal and opposite bending moments.

Figure 17a shows how the most probable position of the rub was identified from best fitting of calculated vibrations to measured ones, by means of the evaluation

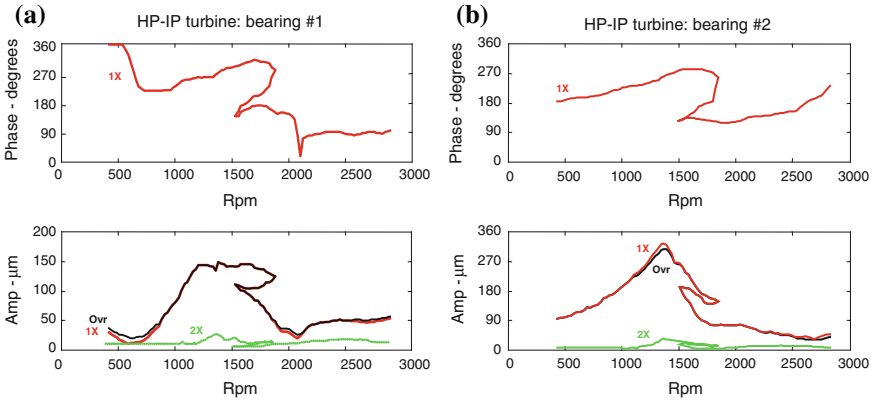

Fig. 15 Interrupted run-down transient of a rubbing steam turbine rotor: stopping at 1,500 rpm, reaccelerating till 1,800 rpm, and completing the run-down: **a** bearing 1; **b** bearing 2

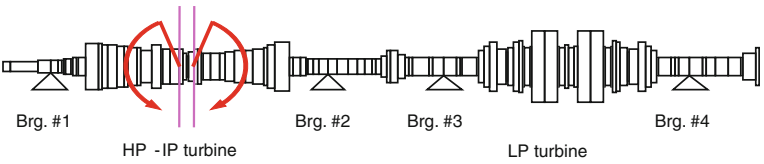

Fig. 16 Fem model of the steam turbine shaft line: bending moments simulate the local thermal bow

of the residues (kind of squared error as vector difference between measured and calculated vibrations) in the model based identification procedure. This has been done in the frequency domain considering stationary conditions at different rotational speed steps. Minimum value of residue identified the most probable position of the rubbing section.

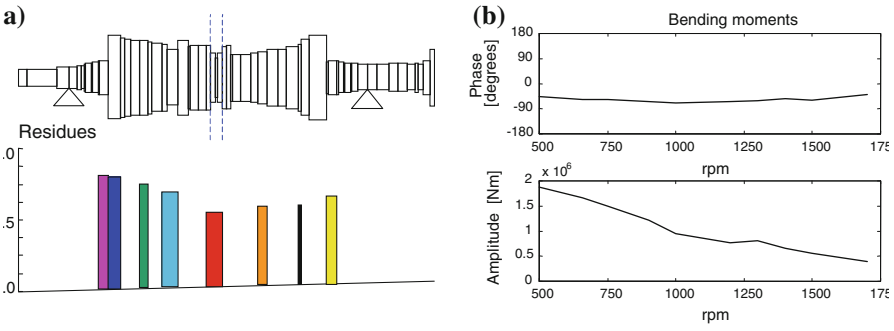

Fig. 17 **a** Most probable location of the rub; **b** Most probable bending moment versus speed

Figure 17b shows the value and phase of the identified bending moment during the run-down transient. Phase is almost constant showing that the contact was not migrating around the shaft circumference, amplitude is increasing showing that the shaft remained in contact with the stator during the whole run-down transient, increasing the developed heat in the same position.

This is again an example where a slowly changing non-stationary condition has been successfully modeled with different steps of stationary conditions, which allowed to remain in the frequency domain, and to use the model based identification procedure in the frequency domain.

8 Experimental Evidence of a Steam Whirl Instability

Instability is a typical strongly non-stationary condition of a rotating machine, which must be overcome rapidly for avoiding failures. Vibrations increase rather suddenly as will be shown in the following case history of a steam whirl instability that occurred in the HP rotor of a 460 MW steam turbine, as described in detail in [6].

These vibrations can be simulated in the frequency domain, taking account of negative damping in the eigen-value of the model of the machine, which defines the rate of the vibration amplitude increase.

Figure 18 represents the sketch of the turbo-group, and Fig. 19 shows a waterfall diagram of the vibration spectra measured in bearing 1 at different time instants before, during and after the event.

In the first part of the diagram the speed (3,000 rpm) is constant, the power (not shown) is increasing. 1xrev. vibration component at 50 Hz is rather low, but a small sub-harmonic component at 32 Hz (first critical speed of the shaft) is present which could indicate an arising instability. At hour 20.42 since power has further increased, suddenly the sub-harmonic component amplitude increases and reaches the shut down level in around 30 s. As the steam inlet valves have been closed, the sub-harmonic component disappears and the speed of the machine decreases. This is the typical symptom of a steam whirl instability, which occurs close to the maximum power (and steam flow) of a turbine. Regarding the modeling the excitation comes from cross coupled stiffness coefficients which develop in blade rows as function of power and clearances, and from steam bearing effect in labyrinth seals as function of the swirl motion. These effects must be taken into account as well as the damping effects of the oil film bearings, for analyzing stability of the machine. The evaluation of these effects are affected by some uncertainties, therefore the design of the machine resulted stable: that means that

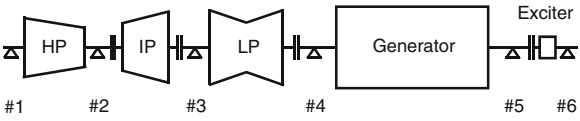

Fig. 18 Sketch of the 460 MW turbo-group where the HP rotor experienced a steam whirl instability

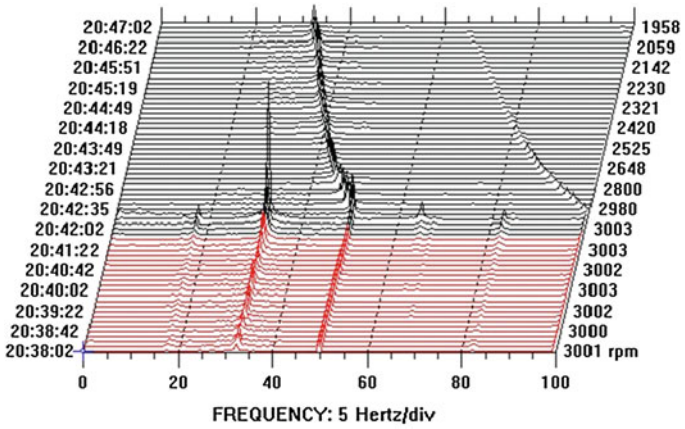

Fig. 19 Waterfall diagram of the vibration spectra measured in bearing 1 of HP rotor during load increase

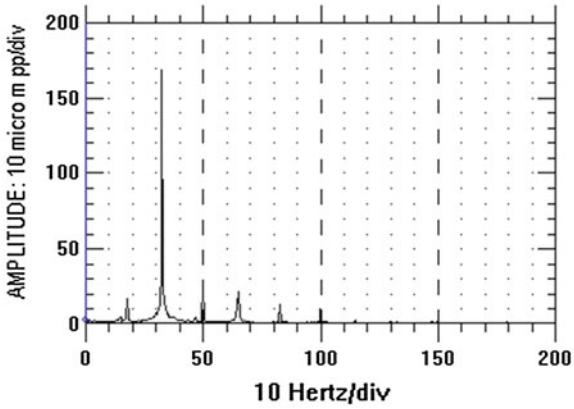

Fig. 20 Vibration spectrum in bearing 1 just before shut-down

the real part of the first eigenvalue of the model of the machine was negative. The measured behavior showed instead a positive value of the real part of the eigenvalue, which was also rather high. Figure 20 shows with more detail one of the spectra recorded during the event.

9 Blade Flutter Instability

This behaviour is described with more detail in [1]. The last stage of the low pressure steam turbine was composed of 120 blades, grouped in packs of 8 blades by welded lashing wires and fixed on the rotor by means of fir tree side entry roots.

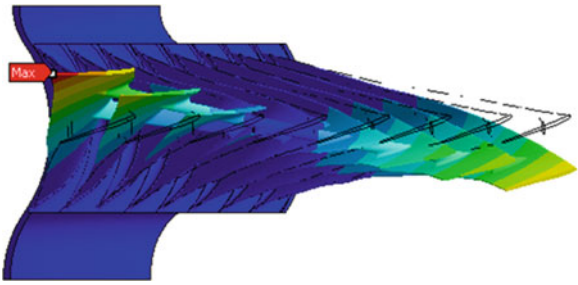

Fig. 21 3rd vibration mode (225 Hz) of the blade pack as calculated from f.e. model modal analysis

During commissioning of the turbine the machine was operated in off design conditions where the long last stage blades may experience high vibrations. An inspection after this period revealed cracks in blade roots and failures in lashing wires. Taking into account also the centrifugal field, the modal analysis allowed to identify the following natural frequencies and associated modes: the 1st (tangential) mode at 115 Hz, the 2nd (axial) mode at 185 Hz and the 3rd (so called X-mode) at 225 Hz. This last mode is shown in Fig. 21 and is the vibration mode that was strongly excited as the cracks and lashing wire failures mostly developed in the first and last blade of the packs. The machine was repaired and equipped with a tip timing blade vibration measuring system. Figure 22 shows the deflections of one blade (blade no. 53) during a speed transient from about 2,700 to 2,890 rpm.

The blade is deflected due to centrifugal force and is vibrating at a frequency of 217 Hz, which is close to one of the natural blade pack frequencies (which resulted to be at 225 Hz at rated speed from calculation). The corresponding pack mode is called X-mode. Resonant conditions could occur at 2,700 rpm with the 5th EO excitation but did not appear. High vibrations are measured instead at a rotational speed of 2,770 rpm, but are not related to the rotational speed (excitation is at a non-integer engine order of 4.7), frequency of vibration is constant and not changing with speed as occurs for the vibrations due to some engine order excitation (that are marked with blue lines in Fig. 22). Vibrations growth and decay depend on some other operating condition parameter, not on speed. Therefore these vibrations must be due to some fluid-dynamic instability. Maximum apparent vibration peak-to-peak amplitude in tangential direction was 14.1 mm, which corresponds to 4.7 mm in the X-mode vibration direction. The fatigue stresses corresponding to similar vibration amplitudes could have caused cracks and failures. Colours which indicate phase of vibration with respect to the 1x rev. reference are randomly distributed around maximum vibration peak, indicating a non-synchronous vibration, where the phase is random. Figure 23 shows the distribution of blade vibrationamplitudes over the blade row composed of 120 blades. The vibration amplitude distribution shows clearly that maximum amplitude exists each 8–9 blades: the first and the last blade of the group of 8 blades are vibrating with maximum amplitude (typical for the X-mode shown in Fig. 21). These blades were also those where cracks close to the roots and lashing wire failures had been

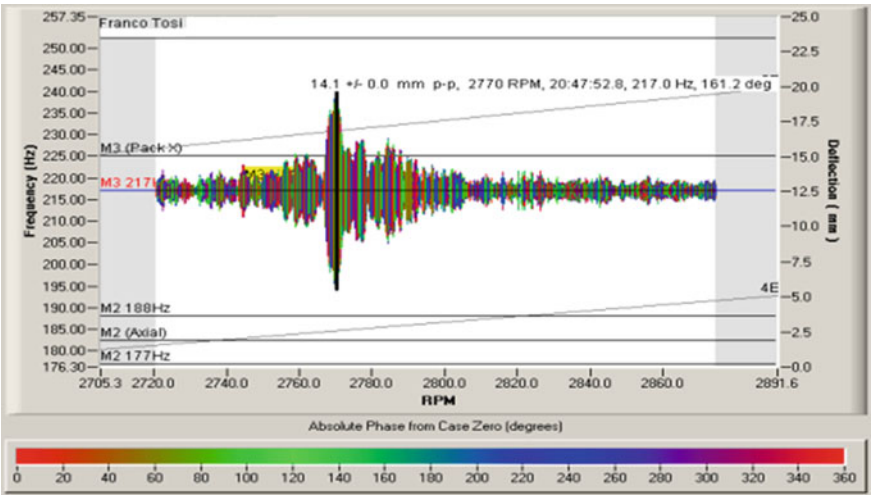

Fig. 22 Transient unstable vibrations of blades during a speed transient of the steam turbine

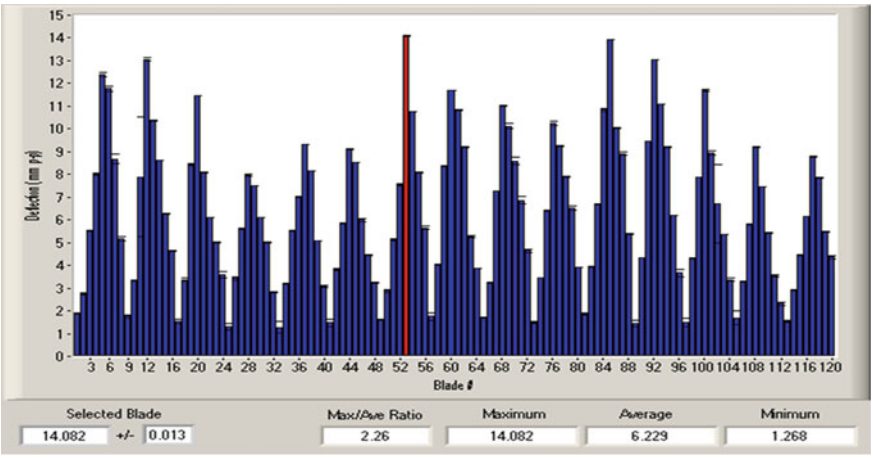

Fig. 23 Vibration amplitude distribution along the blade row during instability

found. In the row of 120 blades there are 15 packs of 8 blades each, therefore 15 peaks and 15 nodes are found in the vibration distribution around the row.

During this non-stationary condition of the machine, small variation in output power and condenser pressure cause apparently the onset of this instability, the evolution over time of the vibrations, with its growth and decays that are extremely difficult to be modeled and cannot be simulated or predicted with sufficient accuracy.

10 Conclusions

The simulation of typical vibration behavior of rotating machines in "weak" or "strong" non-stationary conditions is presented and discussed. The behavior of slowly changing systems (weak non-stationary condition) can be simulated in a mixed approach using both time domain and frequency domain approach. This is the case for instance when the vibration behavior of rotors during thermal transients are simulated. Some experimental results are also presented and compared to simulations. Further examples of systems with strong non-linearity, that in stationary conditions exhibit non-stationary vibrations, are also given. Finally two strong non-stationary instability conditions (cases 8 and 9) are presented of rotating shafts and blade rows: the first one can be simulated rather easily with a linear model, the latter is very difficult to be simulated.

References

1. SanvitoM, Pesatori E, Bachschmid N, Chatterton S (2012) Analysis of LP steam turbine blade vibrations: experimental results and numerical simulations, 10th International conference on vibrations in rotating machinery IMechE, London, pp 11–13
2. Bachschmid N, Pennacchi P, Pesatori E, Turozzi G (2007) On the "snubbing" mechanism for reducing blade vibration, proceedings of the ASME international design engineering technical conferences and computers and information in engineering conference, DETC2007, 1261–1270
3. Ferrante M, Pesatori E, Bachschmid N (2012) Simulation of the dynamic behavior of a group of blades with friction contacts, 10th international conference on vibrations in rotating machinery IMechE, London, 11–13
4. Bachschmid N, Pennacchi P, Vania A (2000) Modeling of spiral vibrations due to rub in real rotors, 7th international conference on vibrations in rotating machinery IMechE, C576/082
5. Vania A, Bachschmid N, Pennacchi P (2001) Analysis of light rotor-to-stator contacts in large turbine-generator units, 4th International conference on acoustical and vibratory surveillance methods and diagnostic techniques, Compiègne, France
6. Bachschmid N, Pennacchi P, Vania A (2007) Some results in steam whirl analysis, 12th IFToMM world congress, Besançon, France, 18–21